International Journal of Fracture **127:** 167–191, 2004.

Variations of stress intensity factor of a semi-elliptical surface crack subjected to mixed mode loading

NAO-AKI NODA, TOSHIAKI KIHARA and DAISUKE BEPPU
Department of Mechanical Engineering, Kyushu Institute of Technology, 1-1, Sensui-cho, Tobata, Kitakyushu 804-8550, Japan, (E-mail: noda@mech.kyutech.ac.jp)

Received 14 March 2001; accepted in revised form 23 March 2004

Abstract. Maximum stress intensity factors of a surface crack usually appear at the deepest point of the crack, or a certain point along crack front near the free surface depending on the aspect ratio of the crack. However, generally it has been difficult to obtain smooth distributions of stress intensity factors along the crack front accurately due to the effect of corner point singularity. It is known that the stress singularity at a corner point where the front of 3 D cracks intersect free surface is depend on Poisson's ratio and different from the one of ordinary crack. In this paper, a singular integral equation method is applied to calculate the stress intensity factor along crack front of a 3-D semi-elliptical surface crack in a semi-infinite body under mixed mode loading. The body force method is used to formulate the problem as a system of singular integral equations with singularities of the form r^{-3} using the stress field induced by a force doublet in a semi-infinite body as fundamental solution. In the numerical calculation, unknown body force densities are approximated by using fundamental density functions and polynomials. The results show that the present method yields smooth variations of mixed modes stress intensity factors along the crack front accurately. Distributions of stress intensity factors are indicated in tables and figures with varying the elliptical shape and Poisson's ratio.

Key words: Body force method, elasticity, fundamental density, numerical analysis, semi-elliptical surface crack, singular integral equation, stress intensity factor.

Nomenclature

a, b = radius of a semi-elliptical crack
β = parametric angle of ellipse from free surface
ν = poisson's ratio
λ_s = corner point singular index for symmetric deformation
λ_A = corner point singular index for skew-symmetric deformation
$F_{\mathrm{II}}(\beta)$, $F_{\mathrm{III}}(\beta)$ = dimensionless stress intensity factors
$F_{\mathrm{II}E}$, $F_{\mathrm{III}E}(\beta)$ = solution of an elliptical crack

1. Introduction

Surface crack solutions are widely used in applications of fracture mechanics to fatigue and monotonic loadings. Semi-elliptical surface cracks lying perpendicular to the surface in Figure 1 have been used as a fundamental model for actual defects and cracks appearing at the surface of structural components (Raju-Newman, 1979). As shown in Figure 2, maximum stress intensity factors usually appear at the deepest point of the crack, or a certain point near the free surface along crack front depending on the aspect ratio of the crack (Noda-Miyoshi,

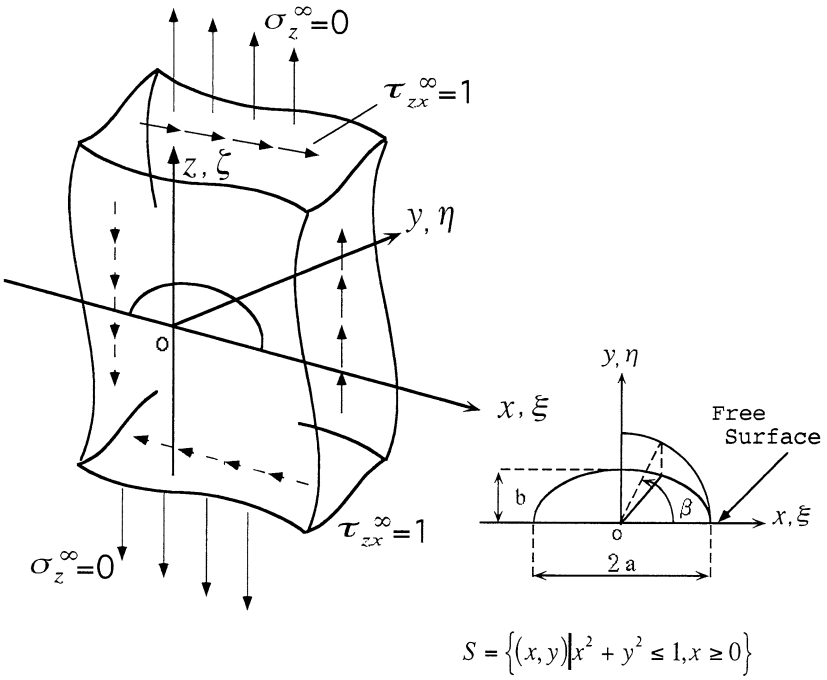

Figure 1. Problem of analysis (a, b = radius of semi-elliptical crack, β = parametric angle from free surface).

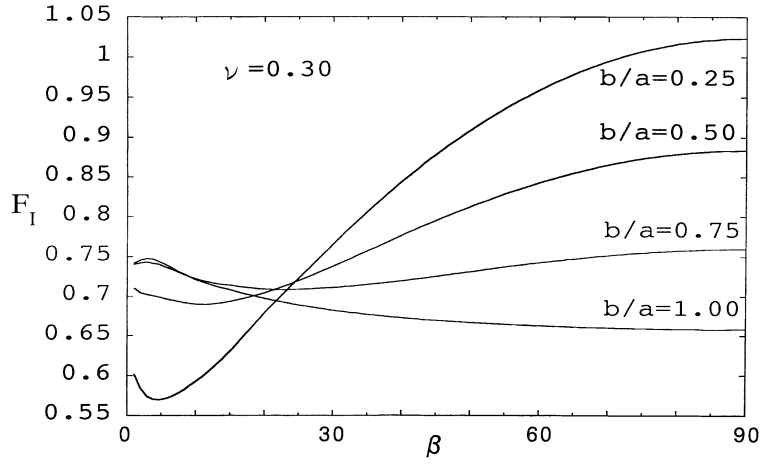

Figure 2. Results of $F_I = K_I/\sigma_z^\infty\sqrt{\pi b}$ for a semi-elliptical crack when $\sigma_z^\infty = 1$, $\tau_{zx}^\infty = 0$ and $\nu = 0.3$ in Figure 1.

1996). However, generally it has been difficult to obtain smooth distributions of stress intensity factors along the crack front accurately due to the effect of corner point singularity.

In 3 D surface cracks the point where the front intersects free surface is known as a corner point. Several researchers discussed that the stress singularity at this point is different from the one of ordinary crack, that is, $r^{-0.5}$ (Bazant, 1974; Bazant-Estenssoro, 1977; Benthem, 1979; Fujitani, 1980; Barsoum, 1988; Nakamura-Parks, 1988, 1989; Ghahremani-Shih,1992; Pook, 1992, 1994; Dhondt, 1998). Also, Benthem (1977, 1980), Bazant-Estenssoro (1979), Takakuda et al. (1985), and Ghahremani (1991) indicated that the corner point singularities are

expressed as $r^{-\lambda_s}$ or $r^{-\lambda_A}$. Then, the singular indexes vary in the range as $0.5 \geqslant \lambda_s \geqslant 0.332$ for symmetric deformations, and as $0.5 \leqslant \lambda_A \leqslant 0.646$ for skew-symmetric deformations, depending on Poisson's ratio in the range $0 \leqslant \nu \leqslant 0.5$. Murakami-Natsume (2000) also clarified that the stress field of surface cracks is affected by the corner point singularity and therefore the region size controlled by the form $r^{-0.5}$ becomes smaller especially near the surface and goes to zero at the corner point. Recent experimental observation shows that fatigue threshold under mixed mode loading is different from the one under monotonic loading (John et al., 1996, 1999; Campbell et al., 1999); and therefore, accurate distributions of stress intensity factors for surface cracks under mixed mode loadings have been required for detail experimental studies.

In our previous studies, the body force method is used to formulate three-dimensional crack problems as a system of integral equations. In the numerical solutions, unknown body force densities are approximated by using fundamental density functions and polynomials. Then, the method is found to yield highly satisfied boundary conditions within the error of 3×10^{-3} throughout the crack surface (Noda-Miyoshi, 1996; Noda et al., 1999). In this paper, the method is applied to calculate the stress intensity factor along crack front of a 3-D semi-elliptical surface crack under mixed mode loading as shown Figure 1. In previous studies Tohgo-Otsuka-Yuuki (1986), Otsuka-Togho-Yoshida (1988), He-Hutchinson (2000), and Murakami-Natsume (2000) analyzed similar surface cracks under shear loading using finite element methods. The present method is, however, efficient and useful for obtaining accurate and smooth variations of mixed modes stress intensity factors even near free surfaces where corner point singularities appears. Distributions of stress intensity factors will be indicated in tables and figures with varying the elliptical shape and Poisson's ratio.

2. Singular integral equation of the body force method

Consider a semi-infinite body subjected to stresses at infinity $\sigma_z^\infty = 0$, $\tau_{zx}^\infty = 1$. A semi-elliptical crack is assumed to be on the xy-plane as shown in Figure 1. Here, the zx-plane is free from stress. The body force method is used to formulate the problem as a system of singular integral equations, where unknowns are body force densities $f_{yz}(\xi, \eta)$, $f_{zx}(\xi, \eta)$ distributed in a semi-infinite body. Here, (ξ, η, ζ) is a (x, y, z) coordinate where the body force is applied. Equations (1a) and (2b) enforce boundary conditions at the prospective boundary S for crack; that is, $\tau_{yz} = 0$, $\tau_{zx} = 0$. Equation (1) includes singular terms in the from of $1/r_1^3$, $1/r_1^5$ corresponding to the ones of an elliptical crack in an infinite body. The notation $=\!\!\!\!\!\!\iint_s$ should be interpreted as a finite part integral in the region S. The notation $K_{yz}^{f_{zx}}(\xi, \eta, x, y, \psi)$ refers to a function that satisfies the boundary condition for free surface.

$$\left.\begin{aligned}
&\frac{1}{8\pi(1-\nu)}\left[=\!\!\!\!\!\!\iint_s \left\{\frac{2(1-2\nu)}{r_1^3}+\frac{6\nu(y-\eta)^2}{r_1^5}\right\} f_{yz}(\xi,\eta)\mathrm{d}\xi\,\mathrm{d}\eta\right.\\
&+=\!\!\!\!\!\!\iint_s \frac{6\nu(x-\xi)(y-\eta)}{r_1^5} f_{zx}(\xi,\eta)\mathrm{d}\xi\,\mathrm{d}\eta\\
&+\iint_s K_{yz}^{f_{yz}}(\xi,\eta,x,y,\psi) f_{yz}(\xi,\eta)\mathrm{d}\xi\,\mathrm{d}\eta\\
&\left.+\iint_s K_{yz}^{f_{zx}}(\xi,x,y,\psi) f_{zx}(\xi,\eta)\mathrm{d}\xi\,\mathrm{d}\eta\right]=0
\end{aligned}\right\} \tag{1.a}$$

$$\left.\begin{aligned}
&\frac{1}{8\pi(1-\nu)}\left[=\!\!\!\!\!\!\int\!\!\!\!\!\!\int_s \frac{6\nu(x-\xi)(y-\eta)}{r_1^5} f_{yz}(\xi,\eta)\mathrm{d}\xi\,\mathrm{d}\eta\right.\\
&+=\!\!\!\!\!\!\int\!\!\!\!\!\!\int_s \left\{\frac{2(1-2\nu)}{r_1^3}+\frac{6\nu(x-\xi)^2}{r_1^5}\right\} f_{zx}(\xi,\eta)\mathrm{d}\xi\,\mathrm{d}\eta\\
&+\iint_s K_{zx}^{f_{yz}}(\xi,\eta,x,y,\psi) f_{yz}(\xi,\eta)\mathrm{d}\xi\,\mathrm{d}\eta\\
&\left.+\iint_s K_{zx}^{f_{zx}}(\xi,x,y,\psi) f_{zx}(\xi,\eta)\mathrm{d}\xi\,\mathrm{d}\eta\right]=-1
\end{aligned}\right\} \tag{1.b}$$

$$\left.\begin{aligned}
&r_1=\sqrt{(x-\xi)^2+(y-\eta)^2+(z-\zeta)^2}\\
&S=\left\{(\xi,\eta)|(\xi/a)^2+(\eta/b)^2\leqslant 1,\ \eta\geqslant 0\right\}
\end{aligned}\right\} \tag{1.c}$$

$$\left.\begin{aligned}
&x_a=x/a,\qquad y_b=y/b,\\
&U_x(x_a,y_b)=u_x(x_a,y_b+0)-u_x(x_a,y_b-0)=\frac{2(1-\nu)}{E}f_{zx}(x_a,y_b)\\
&U_y(x_a,y_b)=u_y(x_a,y_b+0)-u_y(x_a,y_b-0)=\frac{2(1-\nu)}{E}f_{yz}(x_a,y_b)\\
&U_z(x_a,y_b)=u_z(x_a,y_b+0)-u_z(x_a,y_b-0)=\frac{(1+2\nu)(1+\nu)}{E(1-\nu)}f_{zz}(x_a,y_b)=0
\end{aligned}\right\} \tag{1.d}$$

3. Numerical solutions

In the present analysis, the following expressions have been used to approximate the unknown functions $f_{yz}(\xi,\eta)$, $f_{zx}(\xi,\eta)$ as continuous functions

$$\left.\begin{aligned}
&f_{yz}(\xi,\eta)=F_{yz}(\xi_a,\eta_b)\,w_{yz}(\xi_a,\eta_b)\\
&f_{zx}(\xi,\eta)=F_{zx}(\xi_a,\eta_b)\,w_{zx}(\xi_a,\eta_b)\\
&w_{yz}(\xi_a,\eta_b)=\frac{2b(1-\nu)k^2\tau_{yz0}^{\infty}}{C(k)}\sqrt{1-\xi_a^2-\eta_b^2},\quad \tau_{yz0}^{\infty}=1\\
&w_{zx}(\xi_a,\eta_b)=\frac{2b(1-\nu)k^2\tau_{zx0}^{\infty}}{B(k)}\sqrt{1-\xi_a^2-\eta_b^2},\quad \tau_{zx0}^{\infty}=1\\
&B(k)=\left(k^2-\nu\right)E(k)+\nu k'^2K(k)\\
&C(k)=\left(k^2+\nu k'^2\right)E(k)-\nu k'^2K(k)\\
&k'=b/a\leqslant 1\quad k=\sqrt{1-(b/a)^2}\quad \xi_a=\xi/a\eta_b=\eta/b\\
&K(k)=\int_0^{\pi/2}\frac{d\lambda}{\sqrt{1-k^2\sin^2\lambda}},\quad E(k)=\int_0^{\pi/2}\sqrt{1-k^2\sin^2\lambda}\mathrm{d}\lambda
\end{aligned}\right\} \tag{2}$$

Here, $w_{yz}(\xi_a,\eta_b)$, $w_{zx}(\xi_a,\eta_b)$ are called fundamental density functions, which express the stress field due to an elliptical crack in an infinite body under the stresses τ_{yz}^{∞}, τ_{zx}^{∞} and lead to solutions with high accuracy. In numerical calculations, we can put $\tau_{yz}^{\infty}=\tau_{zx}^{\infty}=1$. Using the expression (2), equation (1.a) is reduced to equation (3), where unknowns are $F_{yz}(\xi_a,\eta_b)$, $F_{zx}(\xi_a,\eta_b)$, which are called weight functions.

$$\left.\begin{aligned}
&\frac{b}{4\pi}\left[\frac{k^2}{C(k)}\iint\!\!\!\!\!\!\diagup_s\left\{\frac{2(1-2\nu)}{r_1^3}+\frac{6\nu(y-\eta)^2}{r_1^5}\right\}F_{yz}(\xi_a,\eta_b)\sqrt{1-\xi_a^2-\eta_b^2}\,\mathrm{d}\xi\,\mathrm{d}\eta\right.\\
&+\frac{k^2}{B(k)}\iint\!\!\!\!\!\!\diagup_s\frac{6\nu(x-\xi)(y-\eta)}{r_1^5}F_{zx}(\xi_a,\eta_b)\sqrt{1-\xi_a^2-\eta_b^2}\,\mathrm{d}\xi\,\mathrm{d}\eta\\
&+\frac{k^2}{C(k)}\iint_s K_{yz}^{f_{yz}}(\xi,\eta,x,y,\psi)F_{yz}(\xi_a,\eta_b)\sqrt{1-\xi_a^2-\eta_b^2}\,\mathrm{d}\xi\,\mathrm{d}\eta\\
&\left.+\frac{k^2}{B(k)}\iint_s K_{yz}^{f_{zx}}(\xi,\eta,x,y,\psi)F_{zx}(\xi_a,\eta_b)\sqrt{1-\xi_a^2-\eta_b^2}\,\mathrm{d}\xi\,\mathrm{d}\eta\right]=0
\end{aligned}\right\}\tag{3}$$

Since the problem is skew-symmetric with respect to y axis, the expression (4) can be applied to approximate unknown functions $F_{yz}(\xi_a,\eta_b)$, $F_{zx}(\xi_a,\eta_b)$.

$$\left.\begin{aligned}
&F_{yz}(\xi_a,\eta_b)=\beta_0\xi_a+\beta_1\xi_a\eta_b\quad+\ldots+\beta_{n-1}\xi_a\eta_b^{n-1}+\beta_n\xi_a\eta_b^n\\
&+\beta_{n+1}\xi_a^{2\times1+1}+\beta_{n+2}\xi_a^{2\times1+1}\eta_b+\ldots+\beta_{2n}\xi_a^{2\times1+1}\eta_b^{n-1}\\
&\quad\vdots\qquad\qquad\vdots\\
&+\beta_{l-2}\xi_a^{2\cdot(n-1)+1}+\beta_{l-1}\xi_a^{2\cdot(n-1)+1}\eta_b\\
&+\beta_l\xi_a^{2\cdot n+1}\\
&=\sum_{i=0}^{l}\beta_i G_i(\xi_a,\eta_b)\\
&F_{zx}(\xi_a,\eta_b)=\gamma_0+\gamma_1\eta_b\quad+\ldots+\gamma_{n-1}\eta_b^{n-1}+\gamma_n\eta_b^n\\
&+\gamma_{n+1}\xi_a^{2\times1}+\gamma_{n+2}\xi_a^{2\times1}\eta_b+\ldots+\gamma_{2n}\xi_a^{2\times1}\eta_b^{n-1}\\
&\quad\vdots\qquad\qquad\vdots\\
&+\gamma_{l-2}\xi_a^{2\cdot(n-1)}+\gamma_{l-1}\xi_a^{2\cdot(n-1)}\eta_b\\
&+\gamma_l\xi_a^{2\cdot n}\\
&=\sum_{i=0}^{l}\gamma_i Q_i(\xi_a,\eta_b)\quad l=\sum_{k=0}^{n}(k+1)=\frac{(n+1)(n+2)}{2}\\
&G_0(\xi_a,\eta_b)=\xi_a,\ G_1(\xi_a,\eta_b)=\xi_a\eta_b,\ldots\\
&\ldots,G_{n+1}(\xi_a,\eta_b)=\xi_a^{2\times1+1},\ldots,G_l(\xi_a,\eta_b)=\xi_a^{2\cdot n+1}\\
&Q_0(\xi_a,\eta_b)=1,\ Q_1(\xi_a,\eta_b)=\eta_b,\ldots\\
&\ldots,Q_{n+1}(\xi_a,\eta_b)=\xi_a^{2\times1},\ldots,Q_l(\xi_a,\eta_b)=\xi_a^{2\cdot n}
\end{aligned}\right\}\tag{4}$$

Using the approximation method mentioned above, we obtain the following system of algebraic equations for the determination of $F_{yz}(\xi_a,\eta_b)$, $F_{zx}(\xi_a,\eta_b)$. The unknown coefficients $\beta_0\sim\beta_l$, $\gamma_0\sim\gamma_l$ $[n=1,2,\ldots1,1=(1/2)(n+1)(n+2)]$ are then determined from Equation (5) by selecting a set of collocation points.

$$\left.\begin{aligned}
&\sum_{i=0}^{l}\left[\beta_i\left(A_{yz,i}^{f_{yz}}+B_{yz,i}^{f_{yz}}\right)+\gamma_i\left(A_{yz,i}^{f_{zx}}+B_{yz,i}^{f_{zx}}\right)\right]=0\\
&\sum_{i=0}^{l}\left[\beta_i\left(A_{zx,i}^{f_{yz}}+B_{zx,i}^{f_{yz}}\right)+\gamma_i\left(A_{zx,i}^{f_{zx}}+B_{zx,i}^{f_{zx}}\right)\right]=-1
\end{aligned}\right\}\tag{5.a}$$

As examples, $A^{f_{yz}}_{yz,i}$, $B^{f_{yz}}_{yz,i}$, $A^{f_{zx}}_{yz,i}$, $B^{f_{zx}}_{yz,i}$ are indicated in Equation (5b).

$$
\left.
\begin{aligned}
B^{f_{zz}}_{yz} &= \frac{b(1-\nu)}{2\pi(1-2\nu)E(k)} \iint_s K^{f_{zz}}_{yz}(\xi,\eta,x,y)G_i\,(\xi_a,\eta_b)\sqrt{1-\xi_a^2-\eta_b^2}\mathrm{d}\xi\,\mathrm{d}\eta \\
A^{f_{yz}}_{yz,i} &= \frac{bk^2}{4\pi C(k)} \oint\!\!\oint_s \left\{\frac{2(1-2\nu)}{r_1^3}+\frac{6\nu(y-\eta)^2}{r_1^5}\right\} G_i\,(\xi_a,\eta_b)\sqrt{1-\xi_a^2-\eta_b^2}\mathrm{d}\xi\,\mathrm{d}\eta \\
B^{f_{yz}}_{yz,i} &= \frac{bk^2}{4\pi C(k)} \iint_s K^{f_{yz}}_{yz}(\xi,\eta,x,y)G_i\,(\xi_a,\eta_b)\sqrt{1-\xi_a^2-\eta_b^2}\mathrm{d}\xi\,\mathrm{d}\eta \\
A^{f_{zx}}_{yz,i} &= \frac{bk^2}{4\pi B(k)} \oint\!\!\oint_s \frac{6\nu(x-\xi)(y-\eta)}{r_1^5} Q_i\,(\xi_a,\eta_b)\sqrt{1-\xi_a^2-\eta_a^2}\mathrm{d}\xi\,\mathrm{d}\eta \\
B^{f_{zx}}_{yz,i} &= \frac{bk^2}{4\pi B(k)} \iint_s K^{f_{zx}}_{yz}(\xi,\eta,x,y)Q_i\,(\xi_a,\eta_b)\sqrt{1-\xi_a^2-\eta_b^2}\mathrm{d}\xi\,\mathrm{d}\eta
\end{aligned}
\right\} \quad (5.b)
$$

In Equation (5b) $B^{f_{yz}}_{yz,i}$, $B^{f_{zx}}_{yz,i}$ can be evaluated easily because of no singularity. However, $A^{f_{yz}}_{yz,i}$, $A^{f_{zx}}_{yz,i}$ have singularities when the point (x, y) coincides with (ξ, η). In this case the integration can be evaluated in a similar way shown in the previous paper (Noda and Miyoshi, 1996).

4. Results and discussion

4.1. Convergence of the results

Numerical calculations have been carried out with varying n in equation (4) when $b/a = 1.0$, 0.75, 2/3, 0.5, 0.25 with Poisson's ratio $\nu = 0$, 0.3, 0.45, 0.5. Numerical integrals (3) and (5) have been evaluated using scientific subroutine library using double-exponential-function-type formula (FACOM SSL II DAQE etc.). In demonstrating the numerical results of stress intensity factors of mode II and mode III the following dimensionless factors will be used. The solution of an elliptical crack, $F_{\mathrm{II}E}(\beta)$ and $F_{\mathrm{III}E}(\beta)$ in equation (6b), is used for comparison (Kassir-Sih, 1966).

$$
\left.
\begin{aligned}
F_{\mathrm{II}}(\beta) &= \frac{K_{\mathrm{II}}(\beta)}{\tau^{\infty}_{zx}\sqrt{\pi b}} = \left(F_{zx}\frac{k'\cos\beta}{B(k)} + F_{yz}\frac{\sin\beta}{C(k)}\right)\frac{k^2}{\left(1-k^2\cos^2\beta\right)^{\frac{1}{4}}} \\
F_{\mathrm{III}}(\beta) &= \frac{K_{\mathrm{III}}(\beta)}{\tau^{\infty}_{zx}\sqrt{\pi b}} = \left(-F_{zx}\frac{\sin\beta}{B(k)} + F_{yz}\frac{k'\cos\beta}{C(k)}\right)\frac{(1-\nu)k^2}{\left(1-k^2\cos^2\beta\right)^{\frac{1}{4}}} \\
F_{yz} &= F_{yz}\,(\xi_a,\eta_b)\,|_{\xi_a=\cos\beta,\eta_b=\sin\beta} \\
F_{zx} &= F_{zx}\,(\xi_a,\eta_b)\,|_{\xi_a=\cos\beta,\eta_b=\sin\beta}
\end{aligned}
\right\} \quad (6.a)
$$

$$
\left.
\begin{aligned}
F_{\mathrm{II}E}(\beta) &= \left(\frac{k'\cos\beta}{B(k)}\right)\frac{k^2}{\left(1-k^2\cos^2\beta\right)^{\frac{1}{4}}} \\
F_{\mathrm{III}E}(\beta) &= \left(\frac{\sin\beta}{B(k)}\right)\frac{(1-\nu)k^2}{\left(1-k^2\cos^2\beta\right)^{\frac{1}{4}}}
\end{aligned}
\right\} \quad (6.b)
$$

Figures 3 and 4 indicates the compliance of the boundary conditions along the prospective crack surface when $b/a = 1.0$ and Poisson's ratio $\nu = 0.3$ with varying n in equation (4). With

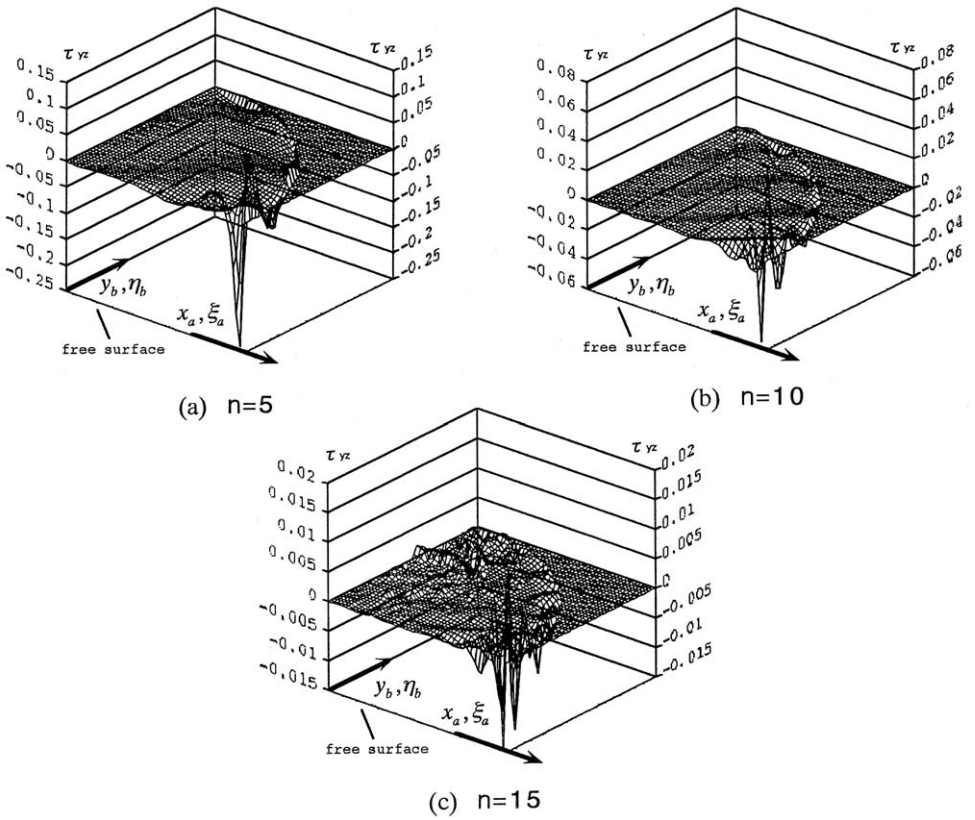

Figure 3. Compliance of boundary condition for $\tau_{yz} \simeq 0$ when $b/a = 1.0$, and $\nu = 0.3$ in Figure 1 when (a) $n = 5$, (b) $n = 10$, (c) $n = 15$.

increasing n the remaining stresses τ_{yz} and τ_{zx} becomes small and less than 1.5×10^{-3} when $n = 15$. Figure 5 also indicates the compliance of the boundary conditions when $b/a = 1.0$ and $n = 20$ with varying r Poisson's ratio ν. With increasing the value of Poisson's ratio, the remaining stress becomes larger due to the strong effect of the corner point singularity. However, the stresses are still less than 2×10^{-3} even in the worst case $\nu = 0.5$ where the corner point singular indexes are $\lambda_s = 0.332$ and $\lambda_A = 0.646$, which are much different from the ones of ordinary cracks, $\lambda = 0.5$.

Table 1 shows the convergence of the present analysis for the worst case of Poisson's ratio $\nu = 0.5$. As shown in Table 1, the results have good convergence to about fourth digit even in the case $\nu = 0.5$.

4.2. Results of a semicircular crack under shear

Table 2 and Figure 6 indicate the results of a semicircular crack for different poisson's ratio in comparison with the results of a penny-shaped crack in an infinite body under shear. As shown in these Table and Figure, F_{II} values are not very different except for the cases $\beta \leqslant 1$, but F_{III} values are much different when $\beta \leqslant 30$ due to the effect of the corner point singularity. With increasing the value of Poisson's ratio, the difference becomes larger due to the strong effect of the corner point singularity because singular index λ_A changes from 0.5 to 0.646 as poisson's

Table 1. Convergence of dimensionless stress intensity factors $F_{\mathrm{II}}(\beta)$, $F_{\mathrm{III}}(\beta)$ when $b/a = 1.0$, $\nu = 0.5$ in Figure 1.

	β(deg)													
	n	1	2	3	4	5	6	7	8	9	10	15	20	25
	17	0.82908	0.78004	0.76479	0.76304	0.76396	0.76304	0.75949	0.75424	0.74861	0.74360	0.72937	0.71054	0.68923
	18	0.83087	0.78181	0.76790	0.76687	0.76745	0.76550	0.76079	0.75470	0.74872	0.74378	0.72965	0.70992	0.68915
F II	19	0.83246	0.78532	0.77369	0.77357	0.77359	0.77021	0.76391	0.75654	0.74978	0.74449	0.72946	0.70972	0.68915
	20	0.83279	0.78589	0.77484	0.77454	0.77369	0.76926	0.76222	0.75458	0.74826	0.74359	0.72957	0.71089	0.69028
	17	0.48543	0.39476	0.34524	0.32111	0.31066	0.30610	0.30303	0.29955	0.29536	0.29098	0.28326	0.28982	0.30072
F III	18	0.47437	0.38785	0.34184	0.32025	0.31126	0.30723	0.30406	0.30017	0.29559	0.29099	0.28397	0.28956	0.30108
	19	0.47410	0.38388	0.33724	0.31643	0.30861	0.30562	0.30317	0.29976	0.29548	0.29111	0.28426	0.28974	0.30179
	20	0.47484	0.38412	0.33779	0.31753	0.31009	0.30712	0.30437	0.30047	0.29569	0.29096	0.28453	0.28944	0.30087
	β(deg)													
	n	30	35	40	45	50	55	60	65	70	75	80	85	90
	17	0.66114	0.62816	0.58951	0.54592	0.49804	0.44558	0.38901	0.32925	0.26702	0.20212	0.13589	0.06785	0.00000
	18	0.66095	0.62827	0.58938	0.54617	0.49770	0.44550	0.38914	0.32926	0.26693	0.20209	0.13593	0.06774	0.00000
F II	19	0.66092	0.62827	0.58936	0.54632	0.49783	0.44551	0.38924	0.32953	0.26679	0.20222	0.13573	0.06808	0.00000
	20	0.66099	0.62830	0.58939	0.54638	0.49772	0.44556	0.38910	0.32945	0.26679	0.20230	0.13567	0.06826	0.00000
	17	0.31806	0.33562	0.35456	0.37304	0.39136	0.40798	0.42319	0.43664	0.44773	0.45697	0.46332	0.46688	0.46811
	18	0.31812	0.33567	0.35449	0.37291	0.39097	0.40759	0.42325	0.43650	0.44780	0.45686	0.46314	0.46633	0.46886
F III	19	0.31809	0.33580	0.35439	0.37331	0.39112	0.40761	0.42320	0.43644	0.44775	0.45672	0.46283	0.46495	0.46487
	20	0.31786	0.33584	0.35440	0.37348	0.39111	0.40769	0.42314	0.43656	0.44769	0.45676	0.46298	0.46551	0.46615

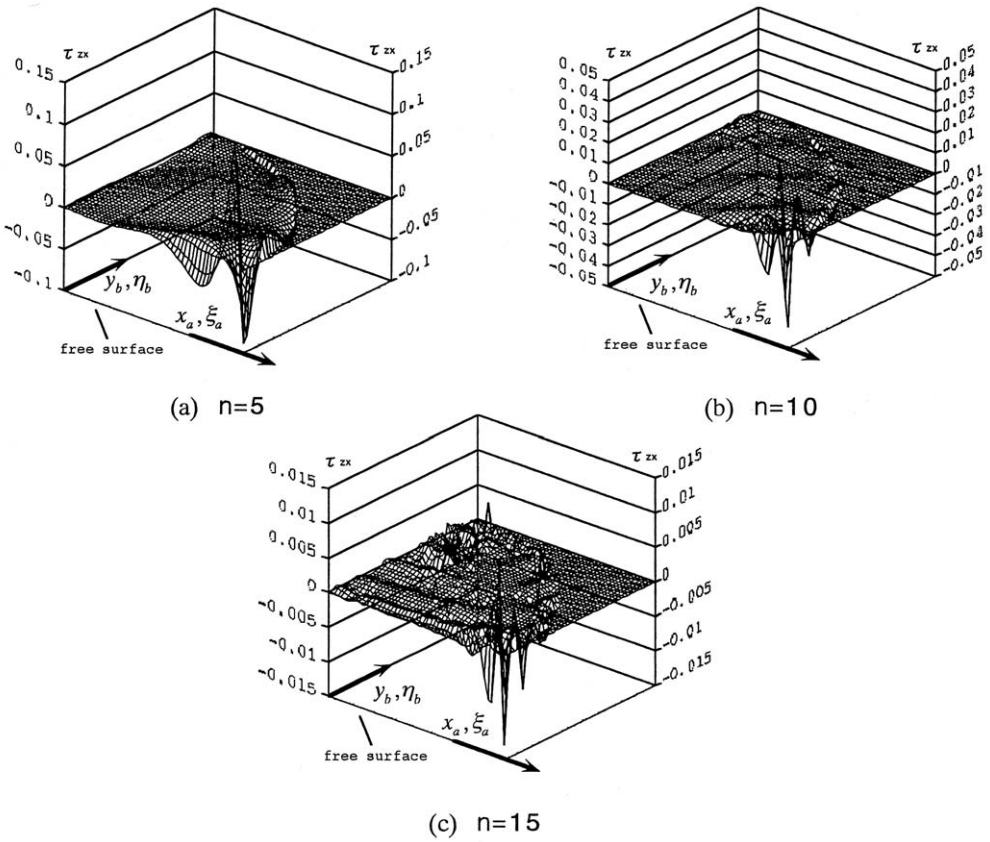

Figure 4. Compliance of boundary condition for $\tau_{zx} \simeq 0$ when $b/a = 1.0$, and $\nu = 0.3$ in Figure 1 when (a) $n = 5$, (b) $n = 10$, (c) $n = 15$.

ratio changes from 0 to 0.5. As shown in Figure 7 the present results and He-Hutchinson's FEM results are in very good agreement when $\nu = 0$.

4.3. Results of a semi-elliptical crack under shear

Tables 3 and 4 indicate the results of semi-elliptical crack under shear for several elliptical ratio b/a when $\nu = 0$, 0.3. When $\nu = 0.3$ the results are plotted in Figure 8. In this case also the solution of an elliptical crack embedded in an infinite body under shear may be used for approximation except near the surface. As shown in Figure 7(b) the mode III stress intensity factor K_{III} does not go to zero smoothly as $\beta \to 0$ when $\nu \neq 0$ although K_{III} value should be zero at $\beta = 0$ (Murakami-Natsume, 2000). In Figure 9, for $\nu = 0.3$ present results and He-Hutchinson's FEM results are also in very good agreement except for F_{II} in the case of $\beta \leqslant 10$.

4.4. Results of a semi-elliptical crack under tension

In the previous paper (Noda-Miyoshi, 1996), a semi-elliptical crack under tension (see Figure 1 with $\sigma_z^{\infty} = 1$, $\tau_{zx}^{\infty} = 0$) has been already treated. However, in order to demonstrate solutions under mixed mode loading, the tensile results are indicated again for the same

Table 2. Results of a semicircular crack $b/a = 1.0$ when $\nu = 0.0, 0.3, 0.45, 0.5$ in Figure 1. [(): Results of a penny shaped crack].

	β(deg)														
	ν	0	1	2	3	4	5	6	7	8	9	10	15	20	25
	0.00	∞	0.646	0.646	0.646	0.645	0.644	0.644	0.642	0.641	0.640	0.638	0.6261	0.6096	0.5882
		(0.637)	(0.637)	(0.636)	(0.636)	(0.635)	(0.634)	(0.633)	(0.632)	(0.630)	(0.629)	(0.627)	(0.6149)	(0.5982)	(0.5770)
	0.30	∞	0.765	0.744	0.733	0.726	0.720	0.715	0.709	0.704	0.700	0.696	0.6814	0.6635	0.6411
F II		(0.749)	(0.749)	(0.749)	(0.748)	(0.747)	(0.746)	(0.745)	(0.743)	(0.742)	(0.740)	(0.738)	(0.7234)	(0.7038)	(0.6788)
	0.45	∞	0.816	0.777	0.766	0.764	0.761	0.756	0.749	0.742	0.736	0.731	0.7165	0.6980	0.6768
		(0.821)	(0.821)	(0.821)	(0.820)	(0.819)	(0.818)	(0.817)	(0.815)	(0.813)	(0.811)	(0.809)	(0.7935)	(0.7719)	(0.7445)
	0.50	∞	0.833	0.786	0.775	0.775	0.774	0.769	0.762	0.755	0.748	0.745	0.7296	0.7109	0.6903
		(0.849)	(0.849)	(0.848)	(0.848)	(0.846)	(0.846)	(0.844)	(0.842)	(0.841)	(0.838)	(0.836)	(0.8199)	(0.7976)	(0.7693)
	0.00	0.000	0.000	0.009	0.019	0.029	0.040	0.051	0.062	0.073	0.084	0.095	0.1499	0.2043	0.2573
		(0.000)	(0.011)	(0.022)	(0.033)	(0.044)	(0.055)	(0.067)	(0.078)	(0.089)	(0.100)	(0.111)	(0.1648)	(0.2177)	(0.2690)
	0.30	0.000	0.284	0.238	0.216	0.208	0.206	0.206	0.206	0.206	0.207	0.208	0.2263	0.2509	0.2804
F III		(0.000)	(0.009)	(0.018)	(0.027)	(0.037)	(0.046)	(0.055)	(0.064)	(0.073)	(0.082)	(0.091)	(0.1357)	(0.1793)	(0.2216)
	0.45	0.000	0.437	0.356	0.315	0.297	0.290	0.286	0.282	0.278	0.274	0.270	0.2695	0.2791	0.2951
		(0.000)	(0.008)	(0.016)	(0.024)	(0.032)	(0.039)	(0.047)	(0.055)	(0.063)	(0.071)	(0.078)	(0.1169)	(0.1545)	(0.1909)
	0.50	0.000	0.475	0.384	0.338	0.318	0.310	0.307	0.304	0.300	0.296	0.291	0.2845	0.2894	0.3009
		(0.000)	(0.007)	(0.015)	(0.022)	(0.030)	(0.037)	(0.044)	(0.052)	(0.059)	(0.066)	(0.074)	(0.1098)	(0.1452)	(0.1794)

Table 2. (Continued).

	β(deg) / ν	30	35	40	45	50	55	60	65	70	75	80	85	90
	0.00	0.5623	0.5320	0.4976	0.4594	0.4177	0.3727	0.3249	0.2746	0.2222	0.1682	0.1128	0.0566	0.0000
		(0.5513)	(0.5215)	(0.4877)	(0.4502)	(0.4092)	(0.3652)	(0.3183)	(0.2690)	(0.2177)	(0.1648)	(0.1105)	(0.0555)	(0.0000)
	0.30	0.6139	0.5819	0.5453	0.5042	0.4591	0.4103	0.3580	0.3029	0.2453	0.1858	0.1247	0.0626	0.0000
F II		(0.6486)	(0.6135)	(0.5737)	(0.5296)	(0.4814)	(0.4296)	(0.3745)	(0.3165)	(0.2562)	(0.1938)	(0.1301)	(0.0653)	(0.0000)
	0.45	0.6481	0.6154	0.5773	0.5346	0.4870	0.4357	0.3805	0.3221	0.2609	0.1976	0.1326	0.0665	0.0000
		(0.7114)	(0.6279)	(0.6293)	(0.5808)	(0.5280)	(0.4712)	(0.4107)	(0.3472)	(0.2810)	(0.2126)	(0.1426)	(0.0716)	(0.0000)
	0.50	0.6610	0.6283	0.5894	0.5464	0.4977	0.4456	0.3891	0.3295	0.2668	0.2023	0.1357	0.0683	0.0000
		(0.7351)	(0.6953)	(0.6502)	(0.6002)	(0.5456)	(0.4869)	(0.4244)	(0.3587)	(0.2903)	(0.2197)	(0.1474)	(0.0740)	(0.0000)
	0.00	0.3083	0.3568	0.4024	0.4448	0.4836	0.5185	0.5493	0.5758	0.5977	0.6149	0.6273	0.6348	0.6373
		(0.3183)	(0.3652)	(0.4092)	(0.4502)	(0.4877)	(0.5215)	(0.5513)	(0.5770)	(0.5982)	(0.6149)	(0.6269)	(0.6342)	(0.6366)
	0.30	0.3108	0.3415	0.3716	0.4005	0.4273	0.4519	0.4739	0.4930	0.5088	0.5214	0.5305	0.5355	0.5370
F III		(0.2621)	(0.3007)	(0.3370)	(0.3707)	(0.4016)	(0.4295)	(0.4540)	(0.4752)	(0.4927)	(0.5064)	(0.5163)	(0.5223)	(0.5243)
	0.45	0.3156	0.3370	0.3585	0.3801	0.4002	0.4189	0.4360	0.4510	0.4634	0.4733	0.4804	0.4837	0.4844
		(0.2259)	(0.2591)	(0.2904)	(0.3195)	(0.3461)	(0.3701)	(0.3913)	(0.4095)	(0.4245)	(0.4364)	(0.4449)	(0.4501)	(0.4518)
	0.50	0.3179	0.3358	0.3544	0.3735	0.3911	0.4077	0.4231	0.4366	0.4477	0.4568	0.4630	0.4655	0.4662
		(0.2122)	(0.2434)	(0.2728)	(0.3001)	(0.3251)	(0.3477)	(0.3676)	(0.3846)	(0.3988)	(0.4100)	(0.4180)	(0.4228)	(0.4244)

Table 3. Results of $F_{\mathrm{II}}(\beta)$, $F_{\mathrm{III}}(\beta)$ for a semi-elliptical crack when $\nu = 0.0$ in Figure 1. [(): Results of an elliptical crack].

	β(deg)														
	b/a	0	1	2	3	4	5	6	7	8	9	10	15	20	25
	1.00	∞	0.646	0.646	0.646	0.645	0.644	0.644	0.642	0.641	0.640	0.638	0.6261	0.6096	0.5882
		(0.637)	(0.637)	(0.636)	(0.636)	(0.635)	(0.634)	(0.633)	(0.632)	(0.630)	(0.629)	(0.627)	(0.6149)	(0.5982)	(0.5770)
	0.75	∞	0.634	0.635	0.635	0.634	0.634	0.633	0.631	0.630	0.628	0.626	0.6119	0.5916	0.5658
		(0.627)	(0.627)	(0.626)	(0.626)	(0.625)	(0.624)	(0.622)	(0.620)	(0.618)	(0.616)	(0.614)	(0.5979)	(0.5764)	(0.5500)
F II	2/3	∞	0.624	0.624	0.624	0.624	0.623	0.622	0.621	0.619	0.617	0.615	0.5996	0.5775	0.5498
		(0.618)	(0.617)	(0.617)	(0.616)	(0.615)	(0.614)	(0.612)	(0.610)	(0.608)	(0.605)	(0.603)	(0.5847)	(0.5609)	(0.5322)
	0.5	∞	0.586	0.587	0.587	0.587	0.586	0.585	0.583	0.581	0.589	0.576	0.5555	0.5284	0.4965
		(0.584)	(0.584)	(0.583)	(0.582)	(0.580)	(0.578)	(0.576)	(0.573)	(0.570)	(0.567)	(0.563)	(0.5387)	(0.5089)	(0.4753)
	0.25	∞	0.461	0.461	0.461	0.459	0.457	0.453	0.449	0.443	0.438	0.431	0.3973	0.3621	0.3286
		(0.466)	(0.466)	(0.464)	(0.461)	(0.457)	(0.452)	(0.446)	(0.440)	(0.433)	(0.426)	(0.418)	(0.3785)	(0.3401)	(0.3051)
	1.00	0.000	0.000	0.009	0.019	0.029	0.040	0.051	0.062	0.073	0.084	0.095	0.1499	0.2043	0.2573
		(0.000)	(0.011)	(0.022)	(0.033)	(0.044)	(0.055)	(0.067)	(0.078)	(0.089)	(0.100)	(0.111)	(0.1648)	(0.2177)	(0.2690)
	0.75	0.000	0.000	0.013	0.026	0.039	0.053	0.068	0.082	0.096	0.110	0.125	0.1954	0.2635	0.3280
		(0.000)	(0.015)	(0.029)	(0.044)	(0.058)	(0.073)	(0.087)	(0.102)	(0.116)	(0.130)	(0.144)	(0.2136)	(0.2797)	(0.3419)
F III	2/3	0.000	0.001	0.015	0.030	0.045	0.060	0.076	0.091	0.107	0.123	0.139	0.2157	0.2892	0.3578
		(0.000)	(0.016)	(0.032)	(0.048)	(0.065)	(0.081)	(0.097)	(0.112)	(0.128)	(0.144)	(0.159)	(0.2350)	(0.3062)	(0.3722)
	0.5	0.000	0.003	0.021	0.040	0.059	0.078	0.098	0.117	0.137	0.156	0.176	0.2681	0.3527	0.4286
		(0.000)	(0.020)	(0.041)	(0.061)	(0.081)	(0.101)	(0.121)	(0.141)	(0.160)	(0.179)	(0.198)	(0.2887)	(0.3705)	(0.4433)
	0.25	0.000	0.013	0.044	0.074	0.104	0.134	0.164	0.192	0.220	0.247	0.273	0.3870	0.4804	0.5580
		(0.000)	(0.033)	(0.065)	(0.097)	(0.128)	(0.158)	(0.188)	(0.216)	(0.243)	(0.270)	(0.295)	(0.4057)	(0.4952)	(0.5691)

Table 3. (Continued).

	β(deg)													
	b/a	30	35	40	45	50	55	60	65	70	75	80	85	90
	1.00	0.5623	0.5320	0.4976	0.4594	0.4177	0.3727	0.3249	0.2746	0.2222	0.1682	0.1128	0.0566	0.0000
		(0.5513)	(0.5215)	(0.4877)	(0.4502)	(0.4092)	(0.3652)	(0.3183)	(0.2690)	(0.2177)	(0.1648)	(0.1105)	(0.0555)	(0.0000)
	0.75	0.5354	0.5010	0.4633	0.4229	0.3803	0.3359	0.2902	0.2433	0.1956	0.1472	0.0984	0.0493	0.0000
		(0.5193)	(0.4851)	(0.4479)	(0.4083)	(0.3668)	(0.3237)	(0.2794)	(0.2342)	(0.1881)	(0.1416)	(0.0946)	(0.0474)	(0.0000)
F II	2/3	0.5177	0.4821	0.4438	0.4034	0.3614	0.3182	0.2741	0.2293	0.1840	0.1383	0.0923	0.0462	0.0000
		(0.4997)	(0.4641)	(0.4263)	(0.3868)	(0.3460)	(0.3042)	(0.2617)	(0.2187)	(0.1754)	(0.1318)	(0.0879)	(0.0440)	(0.0000)
	0.5	0.4616	0.4249	0.3871	0.3488	0.3103	0.2715	0.2327	0.1939	0.1551	0.1163	0.0776	0.0388	0.0000
		(0.4396)	(0.4028)	(0.3656)	(0.3283)	(0.2912)	(0.2542)	(0.2174)	(0.1809)	(0.1445)	(0.1082)	(0.0721)	(0.0360)	(0.0000)
	0.25	0.2973	0.2679	0.2402	0.2137	0.1882	0.1634	0.1392	0.1154	0.0920	0.0688	0.0458	0.0228	0.0000
		(0.2735)	(0.2447)	(0.2181)	(0.1931)	(0.1694)	(0.1466)	(0.1246)	(0.1031)	(0.0821)	(0.0613)	(0.0408)	(0.0204)	(0.0000)
	1.00	0.3083	0.3568	0.4024	0.4448	0.4836	0.5185	0.5493	0.5758	0.5977	0.6149	0.6273	0.6348	0.6373
		(0.3183)	(0.3652)	(0.4092)	(0.4502)	(0.4877)	(0.5215)	(0.5513)	(0.5770)	(0.5982)	(0.6149)	(0.6269)	(0.6342)	(0.6366)
	0.75	0.3881	0.4434	0.4937	0.5389	0.5790	0.6141	0.6442	0.6695	0.6900	0.7059	0.7172	0.7240	0.7262
		(0.3998)	(0.4529)	(0.5011)	(0.5444)	(0.5829)	(0.6164)	(0.6453)	(0.6695)	(0.6892)	(0.7044)	(0.7152)	(0.7217)	(0.7239)
F III	2/3	0.4208	0.4779	0.5293	0.5749	0.6150	0.6498	0.6795	0.7043	0.7244	0.7399	0.7509	0.7575	0.7596
		(0.4327)	(0.4875)	(0.5366)	(0.5801)	(0.6184)	(0.6516)	(0.6800)	(0.7036)	(0.7228)	(0.7375)	(0.7480)	(0.7543)	(0.7563)
	0.5	0.4960	0.5553	0.6073	0.6527	0.6921	0.7260	0.7547	0.7785	0.7978	0.8126	0.8231	0.8294	0.8314
		(0.5076)	(0.5641)	(0.6136)	(0.6567)	(0.6940)	(0.7260)	(0.7532)	(0.7758)	(0.7939)	(0.8079)	(0.8178)	(0.8238)	(0.8257)
	0.25	0.6239	0.6805	0.7297	0.7724	0.8094	0.8413	0.8684	0.8910	0.9094	0.9234	0.9334	0.9394	0.9414
		(0.6317)	(0.6854)	(0.7320)	(0.7724)	(0.8075)	(0.8377)	(0.8634)	(0.8848)	(0.9022)	(0.9155)	(0.9250)	(0.9307)	(0.9326)

Table 4. Results of $F_{\mathrm{II}}(\beta)$, $F_{\mathrm{III}}(\beta)$ for a semi-elliptical crack when $\nu = 0.3$ in Figure 1. [(): Results of an elliptical crack].

	β(deg)														
	b/a	0	1	2	3	4	5	6	7	8	9	10	15	20	25
	1.00	∞	0.765	0.744	0.733	0.726	0.720	0.715	0.709	0.704	0.700	0.696	0.6814	0.6635	0.6411
		(0.749)	(0.749)	(0.749)	(0.748)	(0.747)	(0.746)	(0.745)	(0.743)	(0.742)	(0.740)	(0.738)	(0.7234)	(0.7038)	(0.6788)
	0.75	∞	0.780	0.745	0.730	0.725	0.722	0.718	0.713	0.707	0.702	0.697	0.6755	0.6479	0.6177
		(0.766)	(0.766)	(0.766)	(0.765)	(0.764)	(0.762)	(0.760)	(0.758)	(0.756)	(0.753)	(0.750)	(0.7308)	(0.7046)	(0.6723)
F II	2/3	∞	0.779	0.740	0.723	0.716	0.714	0.711	0.704	0.703	0.697	0.691	0.6648	0.6342	0.6000
		(0.767)	(0.766)	(0.766)	(0.765)	(0.763)	(0.762)	(0.760)	(0.757)	(0.755)	(0.751)	(0.748)	(0.7257)	(0.6961)	(0.6606)
	0.5	∞	0.779	0.732	0.707	0.696	0.689	0.685	0.679	0.673	0.666	0.659	0.6217	0.5817	0.5397
		(0.750)	(0.750)	(0.749)	(0.748)	(0.746)	(0.743)	(0.740)	(0.737)	(0.733)	(0.728)	(0.723)	(0.6924)	(0.6541)	(0.6109)
	0.25	∞	0.668	0.627	0.597	0.576	0.560	0.547	0.535	0.524	0.513	0.501	0.4426	0.3912	0.3470
		(0.637)	(0.636)	(0.634)	(0.630)	(0.624)	(0.617)	(0.610)	(0.601)	(0.592)	(0.582)	(0.571)	(0.5169)	(0.4645)	(0.4167)
	1.00	0.000	0.284	0.238	0.216	0.208	0.206	0.206	0.206	0.206	0.207	0.208	0.2263	0.2509	0.2804
		(0.000)	(0.009)	(0.018)	(0.027)	(0.037)	(0.046)	(0.055)	(0.064)	(0.073)	(0.082)	(0.091)	(0.1357)	(0.1793)	(0.2216)
	0.75	0.000	0.302	0.251	0.227	0.219	0.220	0.223	0.228	0.233	0.237	0.242	0.2741	0.3129	0.3531
		(0.000)	(0.012)	(0.025)	(0.037)	(0.050)	(0.062)	(0.075)	(0.087)	(0.099)	(0.111)	(0.123)	(0.1828)	(0.2393)	(0.2926)
F III	2/3	0.000	0.307	0.257	0.232	0.223	0.224	0.229	0.235	0.242	0.248	0.254	0.2931	0.3381	0.3825
		(0.000)	(0.014)	(0.028)	(0.042)	(0.056)	(0.070)	(0.084)	(0.098)	(0.111)	(0.125)	(0.138)	(0.2042)	(0.2660)	(0.3234)
	0.5	0.000	0.311	0.267	0.242	0.233	0.234	0.241	0.251	0.262	0.273	0.284	0.3396	0.3974	0.4511
		(0.000)	(0.018)	(0.037)	(0.055)	(0.091)	(0.091)	(0.109)	(0.109)	(0.144)	(0.162)	(0.179)	(0.2597)	(0.3333)	(0.3988)
	0.25	0.000	0.245	0.244	0.245	0.250	0.260	0.274	0.291	0.309	0.328	0.348	0.4349	0.5090	0.5723
		(0.000)	(0.031)	(0.062)	(0.092)	(0.122)	(0.151)	(0.179)	(0.207)	(0.233)	(0.258)	(0.282)	(0.3878)	(0.4734)	(0.5441)

Table 4. (Continued).

	β(deg)													
	b/a	30	35	40	45	50	55	60	65	70	75	80	85	90
	1.00	0.6139	0.5819	0.5453	0.5042	0.4591	0.4103	0.3580	0.3029	0.2453	0.1858	0.1247	0.0626	0.0000
		(0.6486)	(0.6135)	(0.5737)	(0.5296)	(0.4814)	(0.4296)	(0.3745)	(0.3165)	(0.2562)	(0.1938)	(0.1301)	(0.0653)	(0.0000)
	0.75	0.5826	0.5441	0.5021	0.4578	0.4111	0.3628	0.3132	0.2625	0.2108	0.1586	0.1059	0.0533	0.0000
		(0.6348)	(0.5929)	(0.5475)	(0.4991)	(0.4484)	(0.3957)	(0.3416)	(0.2862)	(0.2300)	(0.1730)	(0.1156)	(0.0579)	(0.0000)
F II	2/3	0.5620	0.5211	0.4779	0.4333	0.3871	0.3400	0.2925	0.2443	0.1957	0.1470	0.0980	0.0492	0.0000
		(0.6202)	(0.5761)	(0.5291)	(0.4801)	(0.4294)	(0.3776)	(0.249)	(0.2715)	(0.2117)	(0.1635)	(0.1091)	(0.0546)	(0.0000)
	0.5	0.4964	0.4528	0.4094	0.3665	0.3241	0.2823	0.2410	0.2002	0.1597	0.1196	0.0798	0.402	0.0000
		(0.5650)	(0.5177)	(0.4699)	(0.4220)	(0.3742)	(0.3267)	(0.2794)	(0.2325)	(0.1857)	(0.1391)	(0.0927)	(0.0463)	(0.0000)
	0.25	0.3086	0.2746	0.2434	0.2149	0.1881	0.1627	0.1381	0.1144	0.0909	0.0682	0.0455	0.0225	0.0000
		(0.3735)	(0.3342)	(0.2978)	(0.2637)	(0.2313)	(0.2003)	(0.1702)	(0.1409)	(0.1121)	(0.0838)	(0.0557)	(0.0278)	(0.0000)
	1.00	0.3108	0.3415	0.3716	0.4005	0.4273	0.4519	0.4739	0.4930	0.5088	0.5214	0.5305	0.5355	0.5370
		(0.2621)	(0.3007)	(0.3370)	(0.3707)	(0.4016)	(0.4295)	(0.4540)	(0.4752)	(0.4927)	(0.5064)	(0.5163)	(0.5223)	(0.5243)
	0.75	0.3926	0.4304	0.4655	0.4977	0.5266	0.5521	0.5743	0.5929	0.6082	0.6200	0.6284	0.6332	0.6348
		(0.3420)	(0.3875)	(0.4288)	(0.4658)	(0.4987)	(0.5275)	(0.5521)	(0.5729)	(0.5897)	(0.6027)	(0.6120)	(0.6175)	(0.6194)
F III	2/3	0.4255	0.4655	0.5022	0.5355	0.5648	0.5906	0.6127	0.6312	0.6464	0.6580	0.6663	0.6714	0.6730
		(0.3760)	(0.4235)	(0.4662)	(0.5040)	(0.5373)	(0.5662)	(0.5908)	(0.6113)	(0.6280)	(0.6408)	(0.6499)	(0.6553)	(0.6571)
	0.5	0.5003	0.5444	0.5836	0.6182	0.6484	0.6746	0.6969	0.7154	0.7305	0.7419	0.7505	0.7554	0.7566
		(0.4567)	(0.5075)	(0.5520)	(0.5908)	(0.6244)	(0.6532)	(0.6776)	(0.6979)	(0.7143)	(0.7269)	(0.7358)	(0.7411)	0.7429
	0.25	0.6269	0.6742	0.7157	0.7521	0.7836	0.8110	0.8343	0.8539	0.8697	0.8821	0.8906	0.8954	0.8970
		(0.6039)	(0.6552)	(0.6997)	(0.7384)	(0.7719)	(0.8008)	(0.8254)	(0.8459)	(0.8624)	(0.8752)	(0.8843)	(0.8897)	(0.8915)

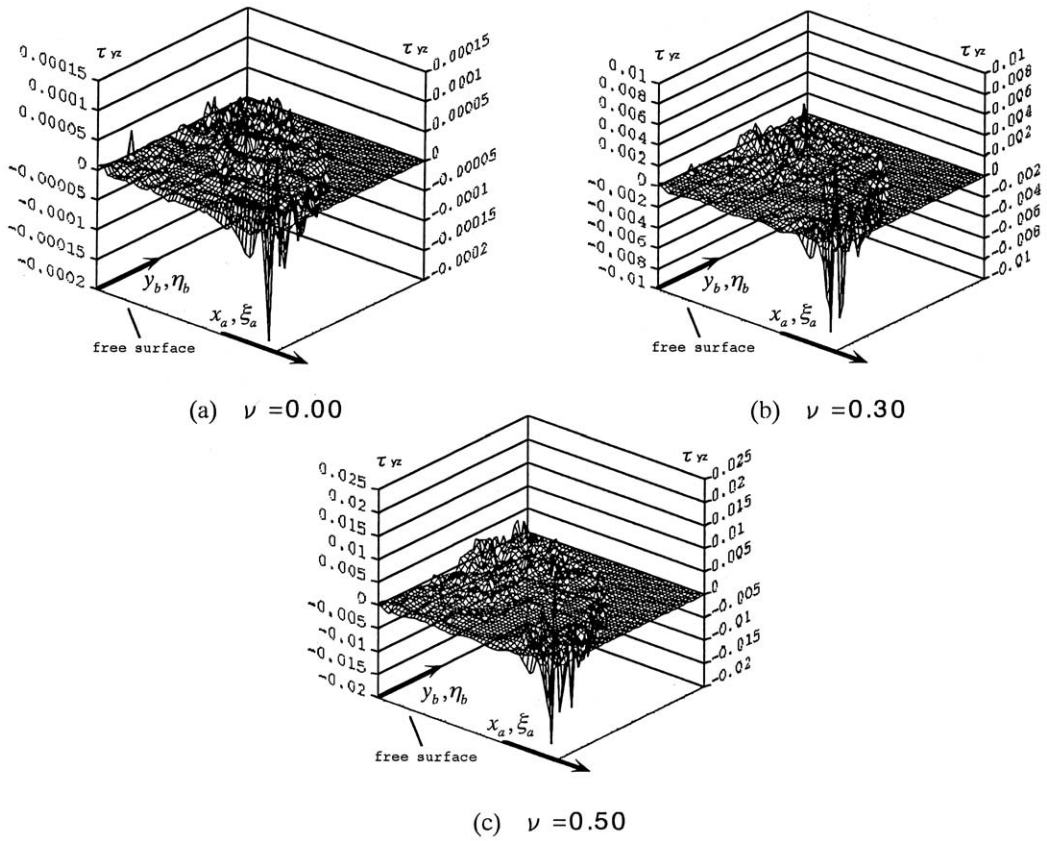

Figure 5. Compliance of boundary condition $\tau_{yz} \simeq 0$ when $b/a = 1.0$, $n = 20$ in Figure 1 when (a) $\nu = 0$, (b) $\nu = 0.3$ (c) $\nu = 0.5$.

aspect ratio and poisson's ratio shown in Tables 2–4. In demonstrating the mode I results the following dimensionless factors will be used.

$$F_{\mathrm{I}}(\beta) = \frac{K_{\mathrm{I}}(\beta)}{\sigma_z^{\infty}\sqrt{\pi b}} \tag{7.a}$$

$$F_{\mathrm{IE}}(\beta) = \left(\frac{1}{E(k)}\right)\left(\sin^2\beta + \left(\frac{b}{a}\right)^2 \cos^2\beta\right)^{1/4} \tag{7.b}$$

Table 5 and Figure 10 indicate the results of a semicircular crack for different poisson's ratio in comparison with the results of a penny-shaped crack in an infinite body under tension. As shown in these Table and Figure, F_{I} value decreases rapidly and goes to zero as $\beta \to 0$. With increasing the value of Poisson's ratio ν from 0 to 0.5, the decrease of F_{I} becomes more rapidly because singular index λ_s changes from 0.5 to 0.332. Tables 6 and 7 indicate the results of a semi-elliptical crack under tension for the same b/a in Table 3, 4.

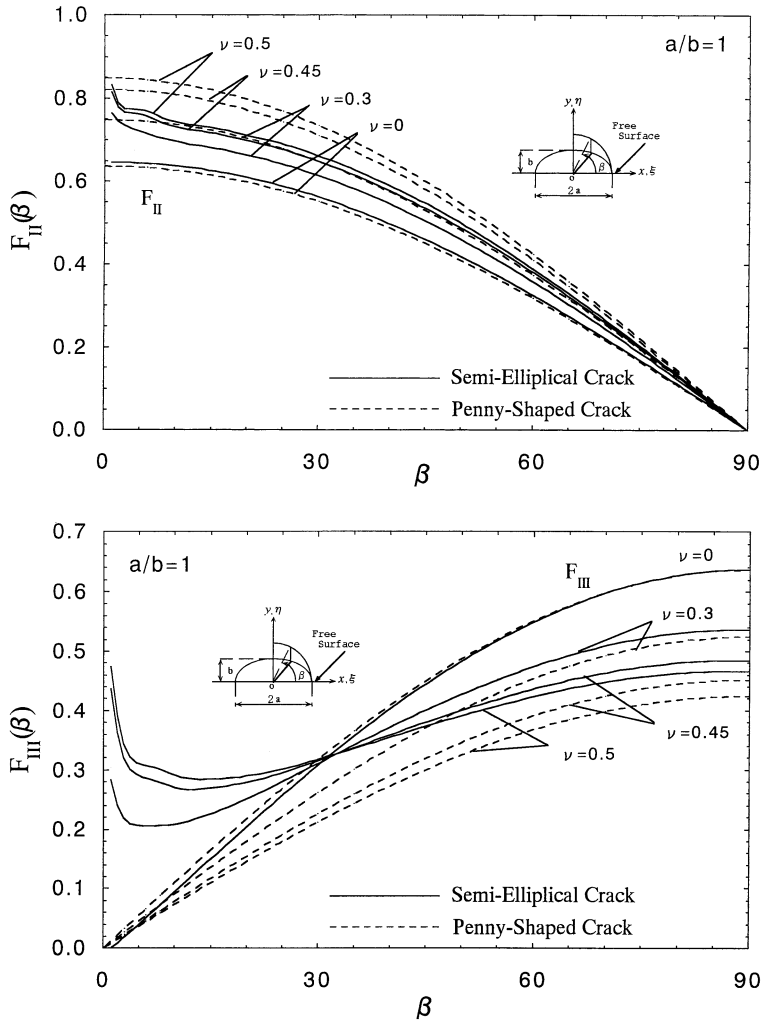

Figure 6. Results of a semicircular crack $b/a = 1.0$ when $\nu = 0.0, 0.3, 0.45, 0.5$ in Figure 1. (a) $F_{\mathrm{II}}(\beta)$ (b) $F_{\mathrm{III}}(\beta)$.

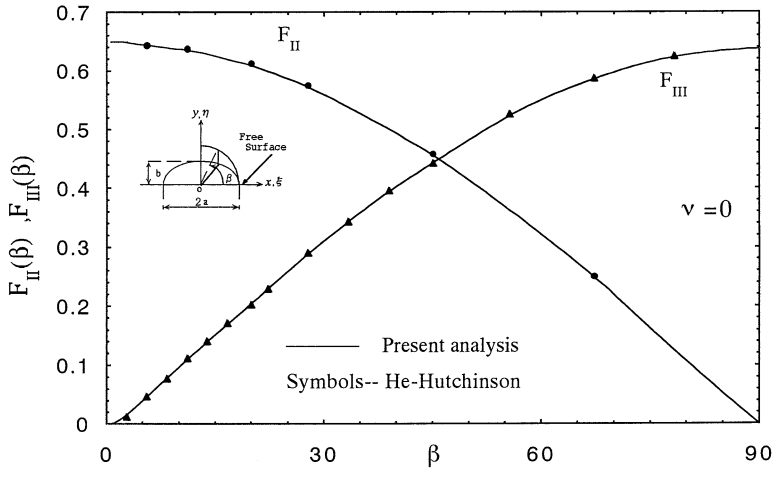

Figure 7. Results of a semicircular crack $b/a = 1.0$ when $\nu = 0.0$ in Figure 1.

Table 5. Results of $F_{\mathrm{I}}(\beta)$ for a semicircular crack $b/a = 1.0$ when $\nu = 0.0, 0.3, 0.45, 0.5$ in Figure 1 when $\sigma_z^{\infty} = 1$, $\tau_{zx}^{\infty} = 0$. [():Results of a penny shaped crack].

	β(deg)														
	ν	0	1	2	3	4	5	6	7	8	9	10	15	20	25
	0.00	0.769	0.752	0.738	0.728	0.720	0.713	0.707	0.701	0.696	0.692	0.688	0.6732	0.6632	0.6562
		(0.6366)	(0.6366)	(0.6366)	(0.6366)	(0.6366)	(0.6366)	(0.6366)	(0.6366)	(0.6366)	(0.6366)	(0.6366)	(0.6366)	(0.6366)	(0.6366)
	0.30	–	0.742	0.746	0.748	0.746	0.742	0.738	0.733	0.729	0.725	0.721	0.7078	0.6969	0.6889
		(0.6366)	(0.6366)	(0.6366)	(0.6366)	(0.6366)	(0.6366)	(0.6366)	(0.6366)	(0.6366)	(0.6366)	(0.6366)	(0.6366)	(0.6366)	(0.6366)
F_{I}	0.45	–	0.707	0.735	0.751	0.757	0.757	0.755	0.752	0.750	0.749	0.747	0.7380	0.7287	0.7192
		(0.6366)	(0.6366)	(0.6366)	(0.6366)	(0.6366)	(0.6366)	(0.6366)	(0.6366)	(0.6366)	(0.6366)	(0.6366)	(0.6366)	(0.6366)	(0.6366)
	0.50	–	0.689	0.726	0.751	0.760	0.762	0.761	0.760	0.759	0.758	0.757	0.7509	0.7427	0.7366
		(0.6366)	(0.6366)	(0.6366)	(0.6366)	(0.6366)	(0.6366)	(0.6366)	(0.6366)	(0.6366)	(0.6366)	(0.6366)	(0.6366)	(0.6366)	(0.6366)

	β(deg)													
	ν	30	35	40	45	50	55	60	65	70	75	80	85	90
	0.00	0.6510	0.6472	0.6442	0.6420	0.6402	0.6388	0.6377	0.6369	0.6363	0.6358	0.6355	0.6353	0.6352
		(0.6366)	(0.6366)	(0.6366)	(0.6366)	(0.6366)	(0.6366)	(0.6366)	(0.6366)	(0.6366)	(0.6366)	(0.6366)	(0.6366)	(0.6366)
	0.30	0.6821	0.6771	0.6729	0.6695	0.6667	0.6645	0.6627	0.6612	0.6601	0.6593	0.6587	0.6582	0.6585
		(0.6366)	(0.6366)	(0.6366)	(0.6366)	(0.6366)	(0.6366)	(0.6366)	(0.6366)	(0.6366)	(0.6366)	(0.6366)	(0.6366)	(0.6366)
F_{I}	0.45	0.7151	0.7099	0.7055	0.7017	0.6986	0.6960	0.6939	0.6922	0.6908	0.6898	0.6891	0.6883	0.6876
		(0.6366)	(0.6366)	(0.6366)	(0.6366)	(0.6366)	(0.6366)	(0.6366)	(0.6366)	(0.6366)	(0.6366)	(0.6366)	(0.6366)	(0.6366)
	0.50	0.7300	0.7248	0.7204	0.7166	0.7134	0.7107	0.7085	0.7067	0.7053	0.7042	0.7035	0.7026	0.7020
		(0.6366)	(0.6366)	(0.6366)	(0.6366)	(0.6366)	(0.6366)	(0.6366)	(0.6366)	(0.6366)	(0.6366)	(0.6366)	(0.6366)	(0.6366)

Table 6. Results of $F_{\mathrm{I}}(\beta)$ for a semi-elliptical crack when $\nu = 0.0$ in Figure 1 when $\sigma_z^{\infty} = 1$, $\tau_{zx}^{\infty} = 0$ [():Results of an elliptical crack].

	β(deg) / b/a	0	1	2	3	4	5	6	7	8	9	10	15	20	25
	1.00	0.769	0.752	0.738	0.728	0.720	0.713	0.707	0.701	0.696	0.692	0.688	0.6732	0.6632	0.6562
		(0.6366)	(0.6366)	(0.6366)	(0.6366)	(0.6366)	(0.6366)	(0.6366)	(0.6366)	(0.6366)	(0.6366)	(0.6366)	(0.6366)	(0.6366)	(0.6366)
	0.75	0.791	0.774	0.755	0.742	0.732	0.724	0.717	0.712	0.707	0.702	0.698	0.6855	0.6798	0.6785
		(0.6269)	(0.6269)	(0.6270)	(0.6272)	(0.6275)	(0.6278)	(0.6282)	(0.6287)	(0.6292)	(0.6298)	(0.6305)	(0.6349)	(0.6407)	(0.6476)
F_{I}	2/3	0.789	0.772	0.742	0.731	0.731	0.723	0.716	0.710	0.705	0.701	0.6973	0.6864	0.6834	0.6854
		(0.6176)	(0.6176)	(0.6178)	(0.6181)	(0.6185)	(0.6190)	(0.6197)	(0.6204)	(0.6213)	(0.6222)	(0.6233)	(0.6301)	(0.6390)	(0.6495)
	0.5	0.783	0.758	0.739	0.725	0.714	0.705	0.699	0.693	0.689	0.686	0.683	0.6798	0.6862	0.6983
		(0.5839)	(0.5840)	(0.5844)	(0.5851)	(0.5860)	(0.5872)	(0.5886)	(0.5903)	(0.5922)	(0.5943)	(0.5967)	(0.6112)	(0.6295)	(0.6500)
	0.25	0.678	0.748	0.628	0.614	0.606	0.601	0.599	0.599	0.601	0.604	0.608	0.6379	0.6764	0.7166
		(0.4633)	(0.4668)	(0.4684)	(0.4710)	(0.4746)	(0.4790)	(0.4843)	(0.4903)	(0.4970)	(0.5042)	(0.5119)	(0.5548)	(0.6007)	(0.6458)

	β(deg) / b/a	30	35	40	45	50	55	60	65	70	75	80	85	90
	1.00	0.6510	0.6472	0.6442	0.6420	0.6402	0.6388	0.6377	0.6369	0.6363	0.6358	0.6355	0.6353	0.6352
		(0.6366)	(0.6366)	(0.6366)	(0.6366)	(0.6366)	(0.6366)	(0.6366)	(0.6366)	(0.6366)	(0.6366)	(0.6366)	(0.6366)	(0.6366)
	0.75	0.6801	0.6837	0.6884	0.6939	0.6996	0.7053	0.7106	0.7155	0.7196	0.7230	0.7254	0.7269	0.7274
		(0.6554)	(0.6636)	(0.6721)	(0.6805)	(0.6887)	(0.6963)	(0.7032)	(0.7093)	(0.7144)	(0.7185)	(0.7215)	(0.7233)	(0.7239)
F_{I}	2/3	0.6906	0.6978	0.7060	0.7148	0.7236	0.7320	0.7397	0.7466	0.7524	0.7570	0.7604	0.7624	0.7631
		(0.6610)	(0.6731)	(0.6853)	(0.6973)	(0.7086)	(0.7191)	(0.7286)	(0.7368)	(0.7437)	(0.7492)	(0.7532)	(0.7555)	(0.7563)
	0.5	0.7135	0.7301	0.7471	0.7637	0.7793	0.7937	0.8065	0.8175	0.8267	0.8339	0.8390	0.8422	0.8433
		(0.6716)	(0.6932)	(0.7143)	(0.7342)	(0.7526)	(0.7693)	(0.7840)	(0.7966)	(0.8070)	(0.8152)	(0.8210)	(0.8245)	(0.8257)
	0.25	0.7553	0.7919	0.8257	0.8563	0.8838	0.9081	0.9292	0.9470	0.9616	0.9728	0.9809	0.9858	0.9874
		(0.6884)	(0.7278)	(0.7537)	(0.7962)	(0.8251)	(0.8504)	(0.8723)	(0.8908)	(0.9059)	(0.9176)	(0.9259)	(0.9309)	(0.9326)

Table 7. Results of $F_{\mathrm{I}}(\beta)$ for a semi-elliptical crack when $\nu = 0.3$ in Figure 1 when $\sigma_z^{\infty} = 1$, $\tau_{zx}^{\infty} = 0$ [():Results of an elliptical crack].

	β(deg)													
	b/a	0	1	2	3	4	5	6	7	8	9	10	15	20	25
	1.00	–	0.742	0.746	0.748	0.746	0.742	0.738	0.733	0.729	0.725	0.721	0.7078	0.6969	0.6889
		(0.6366)	(0.6366)	(0.6366)	(0.6366)	(0.6366)	(0.6366)	(0.6366)	(0.6366)	(0.6366)	(0.6366)	(0.6366)	(0.6366)	(0.6366)	(0.6366)
	0.75	–	0.740	0.742	0.743	0.741	0.739	0.735	0.732	0.728	0.725	0.722	0.7136	0.7091	0.7088
		(0.6269)	(0.6269)	(0.6270)	(0.6272)	(0.6275)	(0.6278)	(0.6282)	(0.6287)	(0.6292)	(0.6298)	(0.6305)	(0.6349)	(0.6407)	(0.6476)
F_{I}	2/3	–	0.737	0.736	0.736	0.736	0.734	0.730	0.726	0.722	0.719	0.716	0.7109	0.7100	0.7139
		(0.6176)	(0.6176)	(0.6178)	(0.6181)	(0.6185)	(0.6190)	(0.6197)	(0.6204)	(0.6213)	(0.6222)	(0.6233)	(0.6301)	(0.6390)	(0.6495)
	0.5	–	0.710	0.704	0.702	0.700	0.698	0.696	0.694	0.692	0.691	0.690	0.6936	0.7044	0.7200
		(0.5839)	(0.5840)	(0.5844)	(0.5851)	(0.5860)	(0.5871)	(0.5886)	(0.5903)	(0.5922)	(0.5943)	(0.5967)	(0.6112)	(0.6295)	(0.6500)
	0.25	–	0.601	0.583	0.573	0.570	0.570	0.572	0.576	0.581	0.587	0.593	0.6315	0.6797	0.7233
		(0.4663)	(0.4668)	(0.4684)	(0.4710)	(0.4746)	(0.4790)	(0.4843)	(0.4903)	(0.4970)	(0.5042)	(0.5119)	(0.5548)	(0.6007)	(0.6458)

	β(deg)													
	b/a	30	35	40	45	50	55	60	65	70	75	80	85	90
	1.00	0.6821	0.6771	0.6729	0.6695	0.6667	0.6645	0.6627	0.6612	0.6601	0.6593	0.6587	0.6582	0.6585
		(0.6366)	(0.6366)	(0.6366)	(0.6366)	(0.6366)	(0.6366)	(0.6366)	(0.6366)	(0.6366)	(0.6366)	(0.6366)	(0.6366)	(0.6366)
	0.75	0.7109	0.7148	0.7197	0.7253	0.7312	0.7370	0.7424	0.7473	0.7515	0.7549	0.7574	0.7592	0.7598
		(0.6554)	(0.6636)	(0.6721)	(0.6805)	(0.6887)	(0.6963)	(0.7032)	(0.7093)	(0.7144)	(0.7185)	(0.7215)	(0.7233)	(0.7239)
FI	2/3	0.7201	0.7284	0.7374	0.7470	0.7563	0.7653	0.7735	0.7808	0.7869	0.7917	0.7953	0.7975	0.7983
		(0.6610)	(0.6731)	(0.6853)	(0.6973)	(0.7086)	(0.7191)	(0.7286)	(0.7368)	(0.7437)	(0.7492)	(0.7532)	(0.7555)	(0.7563)
	0.5	0.7382	0.7574	0.7767	0.7953	0.8128	0.8287	0.8429	0.8552	0.8653	0.8732	0.8788	0.8823	0.8835
		(0.6716)	(0.6932)	(0.7143)	(0.7342)	(0.7526)	(0.7693)	(0.7840)	(0.7966)	(0.8070)	(0.8152)	(0.8210)	(0.8245)	(0.8257)
	0.25	0.7661	0.8069	0.8446	0.8787	0.9092	0.9360	0.9592	0.9789	0.9950	1.0074	1.0162	1.0216	1.0234
		(0.6884)	(0.7278)	(0.7637)	(0.7962)	(0.8251)	(0.8504)	(0.8723)	(0.8908)	(0.9059)	(0.9176)	(0.9259)	(0.9309)	(0.9326)

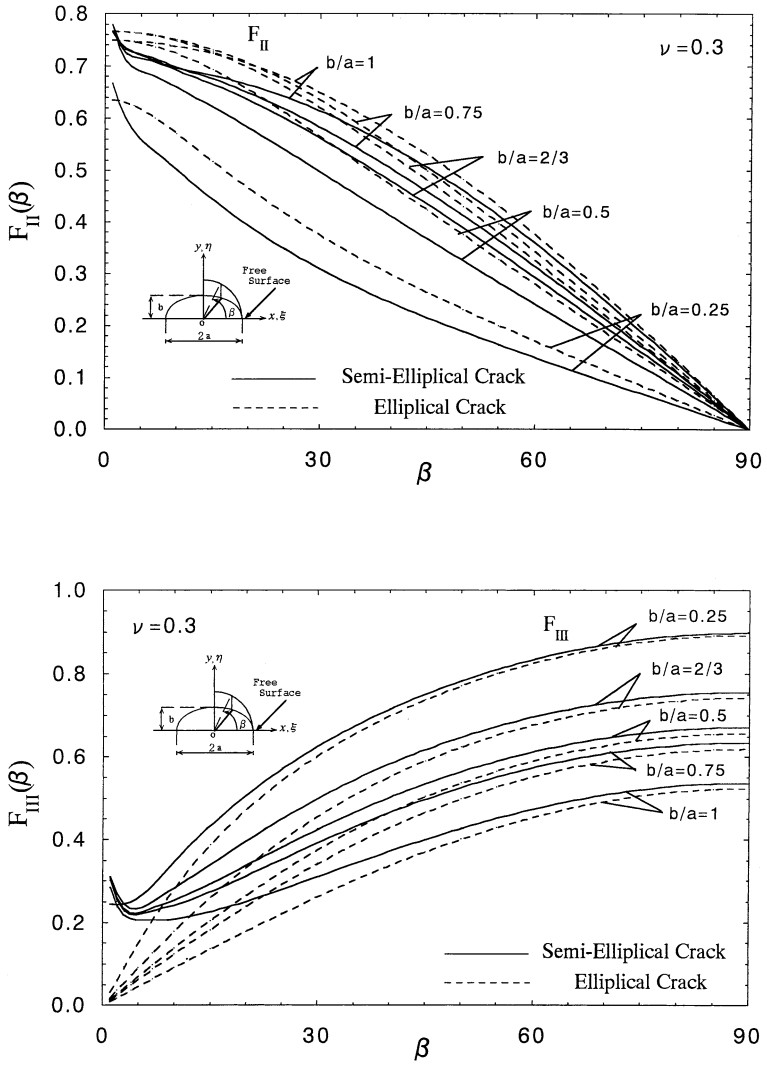

Figure 8. Results of a semi-elliptical crack when $\nu = 0.0$ and $b/a = 1.0, 0.75, 2/3, 0.5, 0.25$ in Figure 1. (a) $F_{II}(\beta)$ (b) $F_{III}(\beta)$.

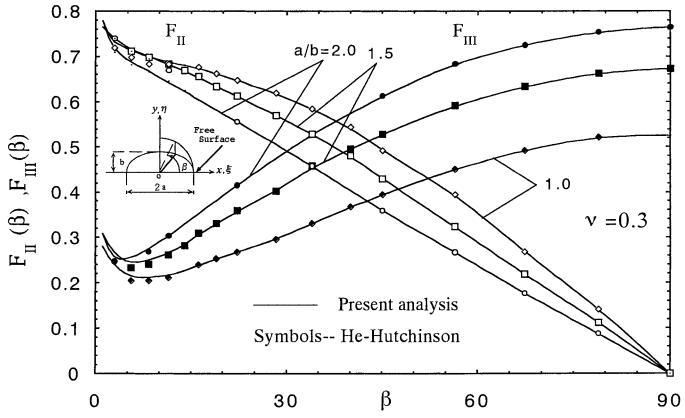

Figure 9. Results of a semi-elliptical crack when $\nu = 0.3$ and $a/b = 1.0, 1.5, 2.0$ in Figure 1. (a) $F_{II}(\beta)$ (b) $F_{III}(\beta)$.

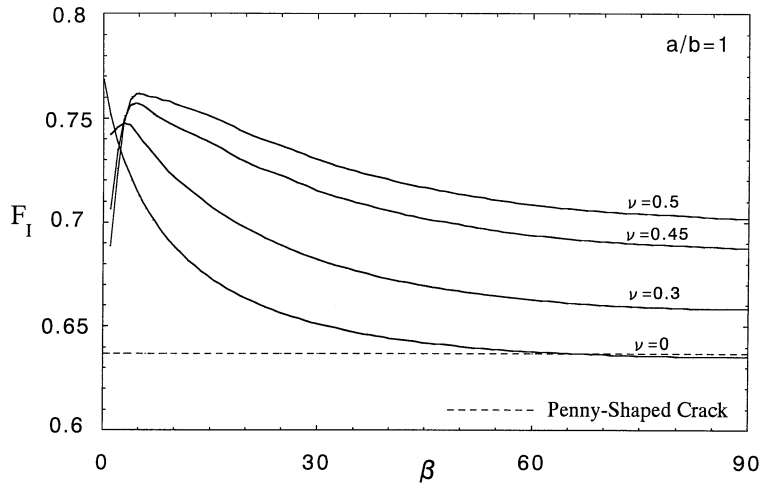

Figure 10. Results of $F_{\mathrm{I}} = K_{\mathrm{I}}/\sigma_z^{\infty}\sqrt{\pi b}$ for a semicircular crack $b/a = 1.0$ when $\sigma_z^{\infty} = 1$, $\tau_{zx}^{\infty} = 0$ in Figure 1.

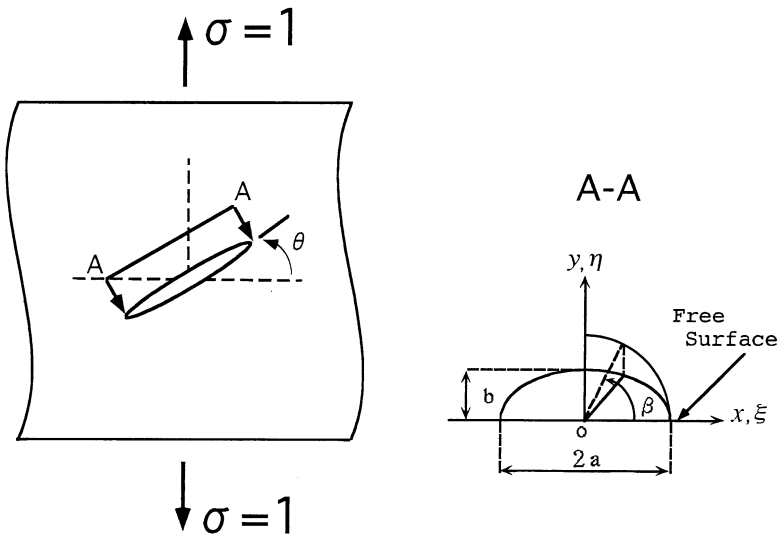

Figure 11. Surface crack aligned obtusely to the remote tensile field.

4.5. Results of a semi-elliptical crack aligned obtusely to the remote tensile field

As an example, the results of a semicircular crack aligned obtusely to the remote tensile field in Figure 11 are indicated in Figure 12. Similar results for different aspect ratio b/a and different Poisson's ratio can be obtained from Tables 2–7.

5. Conclusion

In this paper, a singular integral equation method is applied to calculate the stress intensity factor along crack front of a 3-D semi-elliptical surface crack in a semi-infinite body under mixed mode loading as shown in Figure 1. The body force method is used to formulate the problem as a system of singular integral equations with singularities of the form r^{-3} using the

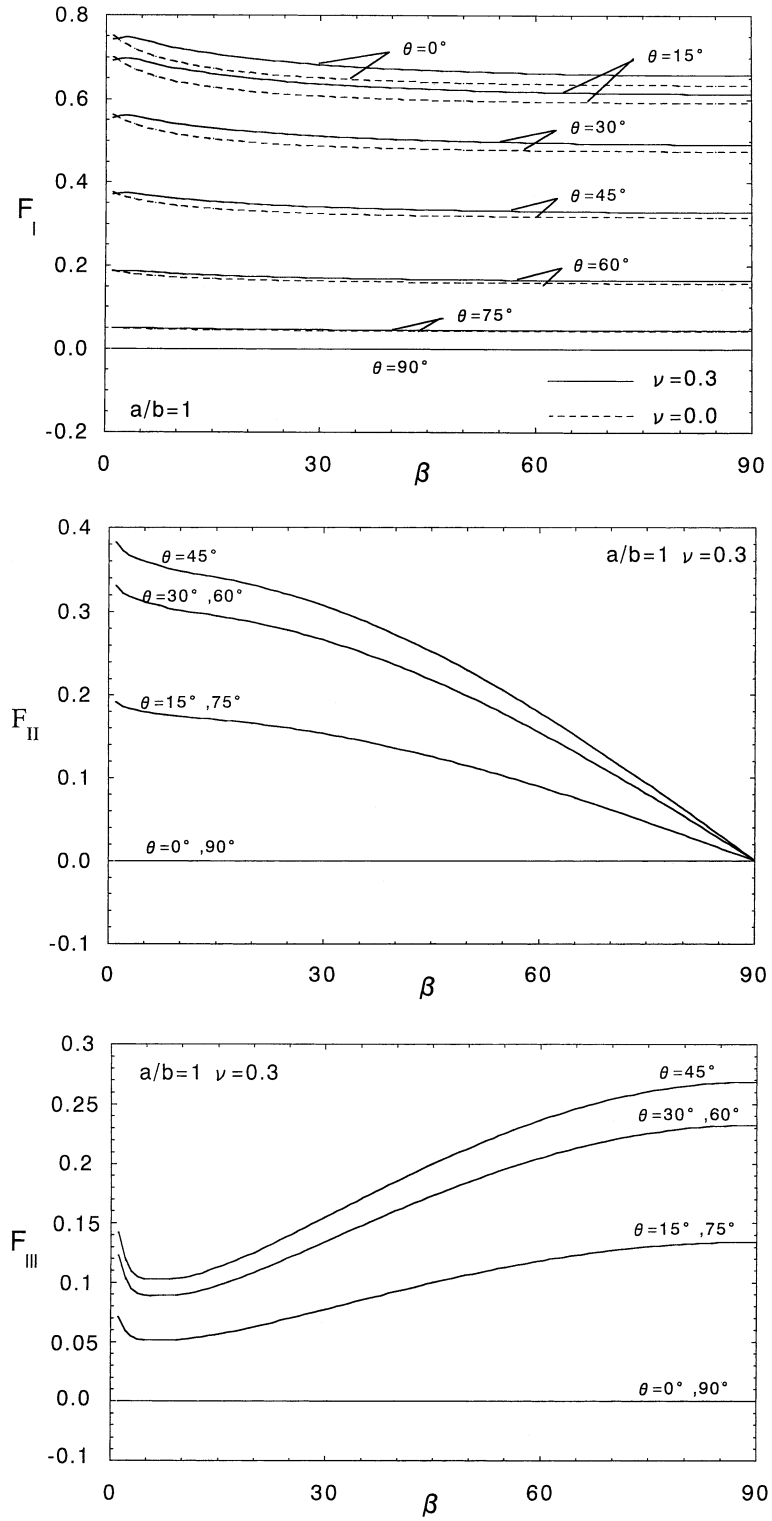

Figure 12. Results of a semicircular crack $b/a = 1.0$ in Figure 10 (a) $F_{\mathrm{I}} = K_{\mathrm{I}}/\sigma_z^{\infty}\sqrt{\pi b}$ (b) $F_{\mathrm{II}} = K_{\mathrm{II}}/\tau_{zx}^{\infty}\sqrt{\pi b}$ (c) $F_{\mathrm{III}} = K_{\mathrm{III}}/\tau_{zx}^{\infty}\sqrt{\pi b}$.

stress field induced by a force doublet in a semi-infinite body as the fundamental solution. The conclusions can be made as follows.

(1) In the numerical calculation, unknown body force densities are approximated by using fundamental density functions and polynomials. The results show that the present method yields highly satisfied boundary conditions throughout the crack boundary.

(2) The present results have good convergence to about fourth digit even when Poisson's ratio $\nu = 0.5$ where the corner point singular indexes are $\lambda_s = 0.332$, $\lambda_A = 0.646$, which are very different from the one of ordinary cracks, $\lambda = 0.5$.

(3) Distributions of stress intensity factors are indicated in tables and figures with varying the elliptical shape and Poisson's ratio for shear, tension, and mixed mode loadings.

(4) The distributions of stress intensity factors of a semi-elliptical crack under shear are very close to the ones of an elliptical crack when $\nu = 0$. However, the deference becomes larger as Poisson's ratio ν becomes large especially near the free surfaces due to the effect of the corner point singularity.

(5) The mode III stress intensity factor K_{III} does not go to zero smoothly as $\beta \to 0$ when $\nu \neq 0$. The present results and He-Hutchinson's FEM results are in very good agreement when $\nu = 0$. For $\nu = 0.3$ present results and He-Hutchinson's FEM results are also in very good agreement except for F_{II} in the case of $\beta \leqslant 10$.

References

Barsoum, R.S. (1988). Application of the finite element iterative method to the eigenvalue problem of a crack between dissimilar media. *International Journal for Numerical Methods in Engineering* **25**, 541–554.

Bazant, Z.P. (1974). Three-dimensional harmonic functions near termination or intersection of gradient singularity line: a general numerical method. *International Journal of Engineering Science* **12**, 221–243.

Bazant, Z.P. and Estenssoro, L.F. (1977). General numerical method for three-dimensional singularities in cracked or notched elastic solids. *Proceedings of the 4th International Conference of Fracture* (Edited by D.M.R. Taplin), Vol.**3**, pp. 371–385, university of Waterloo, Ontario, Canada.

Bazant, Z.P. and Estenssoro, L.F. (1979) Surface singularity and crack propagation. *International Journal of Solids and Structures* **15**, 405–426 (See also Addendum, **16**, 479–481; Erratum **19** 661)

Benthem, J.P. (1977). State of stress at the vertex of crack in a half-space. *International Journal of Solids and Structures* **13**, 479–492.

Benthem, J.P. (1979). On an inversion theorem for conical regions in elasticity theory. *Journal of Elasticity* **9**, 159–169.

Benthem, J.P. (1980). The quarter-infinite crack in a half space; alternative and additional solutions. *International Journal of Solids and Structures* **16**, 119–130.

Campbell, J.P., Thompson, A.W. and Ritchie, R.O. (1999). Mixed-mode crack growth thresholds in Ti-6Al-4V under turbine-engine high cycle fatigue loading conditions. *Proceedings of the 4th National Turbine Engine High Cycle Fatigue Conference* Monterey CA.

Dhondt, G. (1998). On corner point singularities along a quarter circular crack subject to shear loading. *International Journal of Fracture* **89**, L33–L38.

Fujitani, Y. (1980). Analysis of the Stress singular solution in the three-dimensional surface crack problem by Rayleigh-Ritz method, *Bulletin of Hiroshima University* **28**, 129–137 (in Japanese) .

Ghahremani, F. and Shih, C.F. (1992). Corner singularities of three-dimensional planar interface crack. *Journal of Applied Mechanics* **59**, 61–68.

Ghahremani, F. (1991). Numerical variational Method for Extracting 3D Sigularities. *International Journal of Solids and Structures* **27**, 1371–1386.

He, M.Y. and Hutchinson, J.W. (2000). Surface crack subject to mixed mode loading, *Engineering Fracture Mechanics* **65**, 1–14.

John, R., Nicholas, A., Lackey, F. and Porter, W.J. (1996). Mixed-mode crack growth in single crystal Ni-based superalloy. *Fatigue '96, Proceedings of the Sixth International Fatigue Congress* (Edited by G. Lutjering and H. Nowack), Pergamon Press, Oxford, pp. 399–404.

John, R., Deluca, D., Nicholas, T. and Porter, J. (1999). Near-threshold crack growth behavior of a single crystal Ni-based superalloy subjected to mixed-mode loading. *Mixed mode behavior, ASTM STP 1359, ASTM* (Edited by K.J. Miller and D.L. McDowell), West Conshohocken, PA, pp. 312–328.

Kassir, M.K. and Sih, G.C. (1966). Three-dimensional stress distribution around an elliptical crack under arbitrary loadings. *Journal Application Mechanical* **33**, 601–611.

Murakami, Y. and Natsume, H. (2000). Corner point singularity of 3-D crack subjected to mode II loading. *Transactions of the Japan Society of Mechanical Engineers* **66**A, 2211–2217 (in Japanese).

Nakamura, T. and Parks, D.M. (1988). Three-dimensional elastic stress field near the crack front of a thin elastic plate. *Journal of Applied Mechanics* **55**, 805–813.

Nakamura, T. and Parks, D.M. (1989). Anti-symmetrical 3 D stress field near the crack front of a thin elastic plate. *International Journal of Solids and Structures* **25**, 1411–1426.

Noda, N.-A. and Miyoshi, S. (1996). Variation of Stress Intensity Factor and Crack Opening Displacement of a Semi-Elliptical Surface Crack, *International Journal of Fracture* **75**, 19–48.

Noda, N.-A., Kobayashi, K. and Yagishita, M. (1999). Variation of Mixed Modes Stress Intensity Factors of an Inclined Semi-Elliptical Surface Crack, *International Journal of Fracture* **100**, 207–225.

Noda, N.-A., Yagishita, M. and Kihara, H. (2000). Effect of crack shape, inclination angle, and friction coefficient in crack surface contact problems, *International Journal of Fracture* **105**, 367–389.

Otsuka, A., Tohgo, K. and Yoshida, M. (1988). Fatigue crack growth of mixed mode three-dimensional crack (2nd Report, Fatigue crack growth behavior from a semi-elliptical surface crack under shear loading). *Transactions of the Japan Society of Mechanical Engineers* **55**A, 1735–1744 (in Japanese).

Pook, L.P. (1992). A note on corner point singularities. *International Journal of Fracture* **53**, R3–R8.

Pook, L.P. (1994). Some implications of corner point singularities. *Engineering Fracture Mechanics* **48**, 367–378.

Raju, I.S. and Newman, Jr. J.C. (1979). Stress-intensity factors for a wide range of semi-elliptical surface cracks in finite-thickness plates. *Engineering Fracture Mechanics* **11**, 817–829.

Takakuda, K., Koizumi, T. and Sibuya, T. (1985). Stress singularities near crack front edges, *Bulletin of Japan Society of Mechanical Engineers* **28**, 225–231

Tohgo, K., Otsuka, A. and Yuuki, R. (1986). Fatigue crack growth of mixed mode three-dimensional crack (1st Report, Analysis of stress intensity factors of mixed mode three-dimensional cracks based on the J-Integral concept). *Transactions of the Japan Society of Mechanical Engineers* **52**A, 909–918 (in Japanese).